

Overpressure mechanism prediction based on well log and mineralogy analysis from drill cuttings of well NSE-001 in the North Sumatra Basin area, Indonesia

by Aris Buntoro

Submission date: 29-Mar-2022 02:32PM (UTC+0700)

Submission ID: 1795876669

File name: 04_Buntoro_et_al_Journal,_Q2_PEPT_15_March_2022.pdf (2.54M)

Word count: 8407

Character count: 41522



Overpressure mechanism prediction based on well log and mineralogy analysis from drill cuttings of well NSE-001 in the North Sumatra Basin area, Indonesia

Aris Buntoro¹ · Basuki Rahmad² · Dewi Asmorowati¹ · Allen Haryanto Lukmana¹ · Esha Faisal Fattah³ · Edo Anuraga⁴

Received: 15 November 2021 / Accepted: 3 March 2022
© The Author(s) 2022

Abstract

The well NSE-001 is an exploration well located in the North Sumatra Basin, Indonesia, which penetrates several formations with overpressure zones that have the potential as a drilling hazard in this area. The results of the pore pressure fracture gradient model show that the response of the wireline log data of well NSE-001 based on the normal compaction trend has two types of overpressure mechanisms, namely loading and unloading. Rapid sedimentation in the development of the Lower Baong Formation and Upper Baong Formation as thick and massive shale sequences in the North Sumatra Basin is the main factor in the generation of an overpressure zone with a loading mechanism. This correlates with the travel time in the sonic log which is relatively constant with response to the normal compaction trend at depth intervals of 620–1500 mMD (from the Middle Baong Sand Formation to the Top Gebang Sand Formation). The presence of sillimanite and kaliophilite minerals in bulk analysis from drill cuttings at depth intervals of 2200–3820 mMD contributed to the generation of hydrocarbon, while clay analysis showed that the mineral content of kaolinite + illite as alteration product (clay diagenesis) was higher than the mineral content of smectite. The results of the mineralogy analysis (bulk and clay) correlated with the response of the wireline log data of well NSE-001 to the normal compaction trend, which showed that at depth interval of 1500 m to 3200 mMD (from the Top Gebang Sand Formation to the Top Upper Belunai Formation) is an overpressure zone with an unloading mechanism, which was characterized by fluid expansion caused by clay diagenesis and possibly hydrocarbon generation.

Keywords Overpressure mechanism · Well log · Mineralogy · Drill cuttings · North Sumatra Basin

List of symbols

PP	Pore pressure gradient (psi/ft or lb/gal), (kPa/m or g/cc)
OBG	Overburden gradient (psi/ft or lb/gal), (kPa/m, g/cc)
PP _N	Normal pore pressure gradient (psi/ft or lb/gal)
DT _O	Observed interval transit time (msec/m)

DT _N	Normal interval transit time (msec/m)
x	Fracture gradient exponent (dimensionless)
DT	Sonic travel time (microsec/ft, microsec/m)
DT _{ml}	Sonic travel time on V_{max}
A, B, U	Empirical values
V_{max}	The velocity at which unloading occurred for sediments buried at depths
d_{maxv}	Depth at which unloading has occurred
FG	Fracture gradient (psi/ft or lb/gal), (kPa/m or g/cc)
P	Pore pressure
K_i	Matrix stress coefficient (dimensionless)
d	Interplane spacing

Greek symbols

Å	Angstroms
λ	Wavelength X-ray (1.5406 Å)
θ	Diffraction angle
E	Young's modulus (MPa)
ν	Poisson's ratio (dimensionless)

✉ Aris Buntoro
arisbuntoro@upnyk.ac.id

¹ Petroleum Engineering Department, Faculty of Mineral Technology, Universitas Pembangunan Nasional "Veteran", Yogyakarta, Indonesia

² Geological Engineering Department, Faculty of Mineral Technology, Universitas Pembangunan Nasional "Veteran", Yogyakarta, Indonesia

³ Upstream Innovation (UI) - Pertamina Hulu Energi (PHE), Yogyakarta, Indonesia

⁴ Drilling Exploration - Pertamina EP, Yogyakarta, Indonesia

σ Vertical effective stress
 σ_1 Superimposed tectonic stress

Introduction

The North Sumatra Basin is a unique basin, which has high oil and gas potential, but is also an overpressure basin that affects drilling operations. According to Aziz and Bolt (1984) that the top of overpressure is mostly located in the massive shale sequence of the Post-Rift of the Lower Keutapang Formation. The diapir shale is evidence of the presence of overpressure, and indicates a stress regression in the Arun Limestone which lies beneath the Baong Formation under very high pressure. The characteristics of overpressure in the North Sumatra Basin are divided into two overpressure conditions in the Baong Formation, namely the Upper Baong Formation as a mild overpressure zone and the Lower Baong Formation as a high overpressure zone.

From the results of previous studies, an interesting phenomenon was found, namely in several wells in the North Sumatra Basin there were sonic log and resistivity logs reversals, each of which became high sonic and low resistivity (Hutasoit et al. 2013). It is proven that the well drilling in the North Sumatra Basin is in the overpressure zone, although the use of low mud density does not cause significant problems which indicates a mild overpressure zone. This phenomenon can be explained that the shale in the shallow section of hydrostatic pressure has experienced shallow compaction due to under-compacted carbonate cementation in the past, so that the overpressure in the zone is not too high, and is referred to as a mild overpressure zone (Syariful et al 2020).

In identifying the overpressure mechanism in addition to using well log data analysis, it can also be done using mineralogy analysis, namely the hypothesis about the effect of temperature on clay diagenesis that causes the smectite-illite/kaolinite transformation (Storvoll and Brevik 2008; O'Conner et al. 2011).

The drilling target of well NSE-001 is to produce shale gas from the Lower Baong Formation and the Bampo Formation as source rock (Barber et al. 2005; Subroto et al. 2013; Yosandian et al. 2014). The presence of sillimanite mineral, which is brittle mineral due to alteration of clay at high temperatures (600–900 °C), which supports the process of hydrocarbon generation in shale (Buntoro et al. 2020). From the results of XRD analysis (bulk) shows the presence of sillimanite mineral from a depth of 2200 mMD in the Lower Baong Formation as source rock, which is also an overpressure zone.

The discussion in this paper begins by examining the research problem and the hypothesis to be proven. The methodology used in this study is then described, followed

by wireline log response analysis, mineralogy analysis, and analysis of the pore pressure fracture gradient (PPFG) model.

Geology

The North Sumatra Basin contains several oil and gas fields that have drilling problems related to the overpressure zone (Aziz and Bolt 1984). Studies on regional overpressure are still very limited due to the limited data and the variation in the geological conditions of each area (sub-basin). The Baong Formation is a regional reservoir that has many overpressure problems. The sagging tectonic phase in the early Miocene made the sub-basin inundated and became a deep-sea environment. Deep-sea deposits such as shale and claystone are very well developed to form Lower Baong. In the Middle Miocene there was a regional uplift where sandstone deposits were formed which then rapidly subsided to produce fine-grained deposits such as shale and claystone (Upper Baong). The potential overpressure zone is in the Upper Baong Formation and the Lower Baong Formation because it has thick and massive deep-sea shale lithology.

The location of well NSE-001 is in the Tamiang Sub-Basin, North Sumatra Basin, Indonesia (Asset-1 PT. Pertamina EP Area). In the Tamiang Sub-basin the Baong Formation is very well formed. The development of the Lower Baong Formation and the Upper Baong Formation as thick and massive shale sequences is a major factor in the presence of an overpressure zone (Gurning and Ramdhan 2017).

There are two geological factors that may trigger the overpressure zone, namely the loading mechanism caused by rapid sedimentation and the unloading mechanism caused by changes in clay minerals and hydrocarbon generation. However, for hydrocarbon generation, geochemical analysis data of source rock is needed so that it can be more valid.

The North Sumatra Basin is one of the three back arc basins in Sumatra. Regionally, the three basins were formed at the beginning of the Tertiary period with Pre-Tertiary bedrock. The geometry of the North Sumatra Basin tends to be oval with a general direction of Southeast–Northwest and North–South extending eastward to off the coast of Sumatra. This basin is bounded by the Bukit Barisan to the west, the Asahan High to the south-southeast, the Mergui Arc to the north and the Malacca Shelf to the east.

The development and tectonic history of the North Sumatra Basin began in the late Paleozoic-early Mesozoic where the Indo-Australian Plate and the Eurasian Plate were already actively converging. The activity of magmatism and volcanism resulted in the intrusion of granite and granodiorite in Paleozoic and Mesozoic sedimentary rocks to form metamorphic rocks which will act as bedrock. The Indian and Eurasian collisions caused a change in the direction of

subduction from the dominant direction north to northeast so that it was oblique to Sumatra.

According to Pulunggono et al. (1992), there are three tectonic regimes that involve the development of the basin. First, the extensional regime that dominates the basin configuration and early filling from the Late Cretaceous to the early Tertiary. Activities in this regime form a system of graben and horst, which traps and grows from reefs which will later become a hydrocarbon kitchen (kitchen area). Second, the intra Miocene regime that occurred during the Miocene. In this regime, uplift at the edges of the basin is followed by the deposition of clastic sediments. In the latter regime, namely the compressional regime that occurred during the Plio-Pleistocene, it caused an anticlinorium en-echelon pattern, northwest-northwest-east-southeast, and traps were formed. This ended Tertiary deposition in the North Sumatra Basin (Satyana 2009).

The regional stratigraphy of the North Sumatra Basin (Barliana et al. 1999) from oldest to youngest can be seen in Fig. 1. The lithostratigraphic sequence of the North Sumatra Basin from oldest to youngest is as follows: The Tampur Formation consisting of limestone and massive dolomite in

the Late Eocene to Early Oligocene. The Bruksah Formation is interspersed with coarse-grained carbonate sandstones and thin intercalations of coal. The Bampo Formation is dominated by black shale, generally associated with pyrite and calcareous nodules, which were deposited during the Early Miocene. The Peutu Formation consists of claystone and calcareous siltstone which contains many fossils and glauconite of Early Miocene–Middle Miocene age. The Baong Formation consists of shale with sandstone inserts of Middle Miocene age. The Keutapang Formation consists of fine-grained sandstone and shale of Middle Miocene–Upper Miocene age. The Seurula Formation consists of alternating thin layers of sandstone and shale of Early Pliocene age. The Julu Rayeu Formation is an alternation of sandstone, shale, gray clay, tuff, plant remains, and lignite, as well as a small amount of conglomerate of Late Pliocene age.

Based on the explanation of the Regional Tectonic Order and Regional Stratigraphy of the North Sumatra Basin above, it is believed that well NSE-001 is in the Post-Rift to Syn-Rift phase, where in general the folding pattern is in the WNW-ESE direction, forming an en-echelon anticlinorium fold pattern and a horizontal fault (wrench fault). The direction of the horizontal fault movement (wrench fault) is NW–SE according to the basement fault pattern, this is related to the Paleogene graben system (Harding 1974). This condition will cover the blocks that are lifted due to the compression regime of the subduction system, so that the stress that works up to now is Pliocene-Pleistocene stress (Moulds 1989). Thus, it can be concluded that the North Sumatra Basin tectonic is a type of Simple Shear stress (Harding 1974), so that the position of well NSE-001 is believed to have the potential for overpressure, because it is in a simple shear stress system which is influenced by the NS structural pattern with the main stress direction NE–SW (Fig. 2).

Study area

The well NSE-001 is located in the North Sumatra Basin, Indonesia, where the well NSE-001 is an exploration well with a target shale gas reservoir in the Lower Baong Formation and Bampo Formation which are the main source rock in the North Sumatra Basin (Barber et al. 2005; Subroto et al. 2013).

This well was drilled on October 4, 2016, reaching a final depth of 3796.1 mTVD on February 22, 2017. The location of well NSE-001 can be seen in Fig. 3. The following is the formation penetrated in the drilling of well NSE-001 according to the stratigraphy of the North Sumatra Basin from the youngest to the oldest (Fig. 1) as follows:

- Keutapang Formation (0–404 mTVD). The Keutapang Formation consists of fine-grained sandstone and shale.

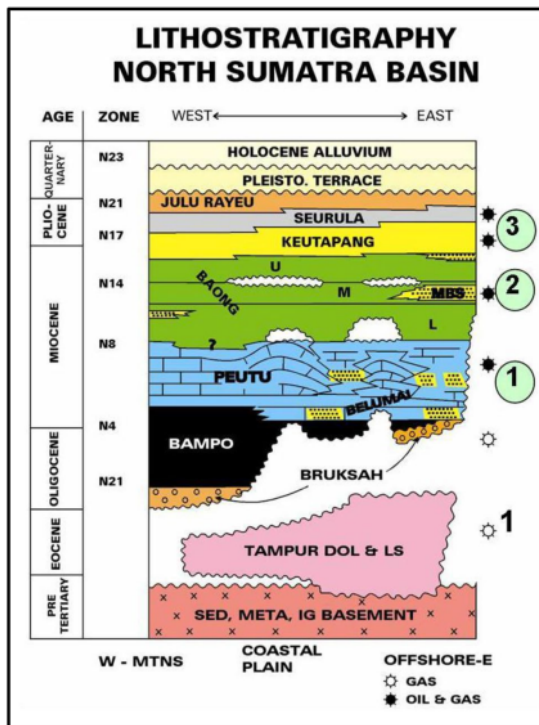


Fig. 1 Chronostratigraphy of the North Sumatra Basin showing the order of deposition from oldest to youngest and from west to east (Barliana et al. 1999)

Fig. 2 Tectonic North Sumatra Basin is a type of simple shear stress (Harding, 1974). The well NSE-001 is strongly influenced by the N-S pattern with the main stress direction NE-SW (N 020 E-N 060 E) and (N 200 E-N 240 E)

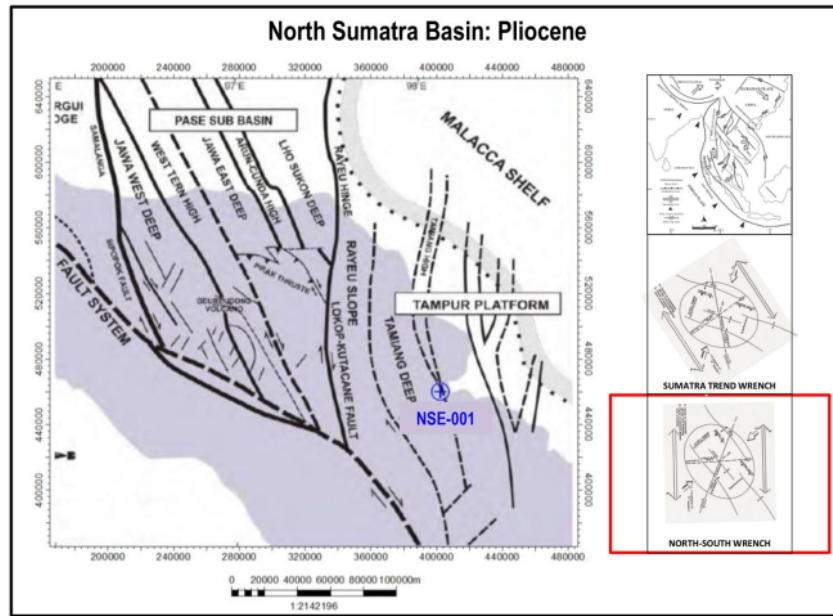
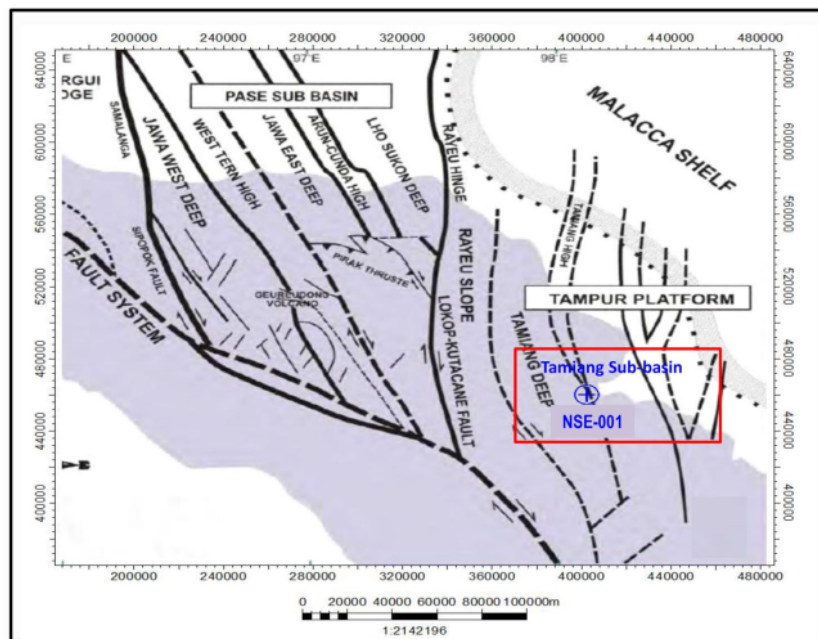


Fig. 3 Location of well NSE-001 (Modified from Harding, 1974)



- Baong Formation (404–3254.6 mTVD). The Baong Formation is dominated by shale with sandstone intercalation. At this depth interval there is a Top Besitang River Sand (BRS) Formation at a depth of 1357.6–1499.1 mTVD with a lithology that is dominated by shale with sandstone and carbonate intercalation. There is a

Top Gebang Formation of 1499.1–2615.6 mTVD with a lithology that is dominated by shale with insertions of sandstone, siltstone, and carbonate.

- Belumai Formation (3254.6–3520.4 mTVD). The Belumai Formation consists of shale and thick layers of limestone and sandstone inserts.

- Bampo Formation (3520.4–3796.1 mTVD). The Bampo Formation consists of shale with little carbonate rock intercalation.

The lithology penetrated in drilling of well NSE-001 is dominated by shale rock types, with some formations found in sandstone and carbonate rock lithology.

Literature review

Pore pressure fracture gradient (PPFG) model prediction method

Many correlations and models have been developed for the prediction of abnormal pressure of various parameters (Hottman and Johnson 1965; Matthews, W.R. and Kelly 1967; Pennebaker 1968; McClendon 1971; Zamora 1974; Eaton 1975). The method has limitations; for example, some models can only be used in clean shales (Table 1).

Some pore pressure prediction methods only can be applied to the pressure generated by the under-compaction mechanism or some of them do not apply in unloading formations. Therefore, the researchers tried to use AI (Acoustic Impedance) from seismic data to predict pore pressure with good precision. To predict the pore pressure, four input parameters are used, namely: depth, Gamma Ray log, density log, and sonic log.

From some literature shows that the parameters used to predict pore pressure from well log data. Most methods require both normal and abnormal trends, to estimate pore pressures.

Overburden gradient prediction calculation

The formation overburden stress gradient (OBG) in onshore drilling can be estimated to vary from 1.0 to 1.1 psi/ft (0.0227–0.025 MPa/m). But in this study, OBG was calculated from the density log (RHOB) data. Because the density log data do not start from the surface/seabed, so in some

Table 1 The pore pressure prediction method can only be used for clean shales (Basuki 2019)

Pore Pressure		
Lithology	Prediction	Measure
Sand	✗	✓
Carbonates	✗	✓
Shale	✓	✗
Salt	✗	✗

equations to calculate the pseudo-RHOB shallow section by integrating the LWD/wireline RHOB log data.

Pore pressure (PP) prediction calculation

There are several methods for predicting pore pressure calculations, namely: Equivalent Depth, Eaton’s, and Bower’s methods.

Eaton’s method:

In the prediction of the pore pressure of well NSE-001 using the Eaton’s method, where Eaton’s exponent which is matched with the actual MW is 3.5 (Eaton’s exp: 3.5). Mathematical equation Eaton’s method used:

$$PP = OBG - (OBG - PP_N) \left(\frac{DT_N}{DT_O} \right)^x \tag{1}$$

where PP = Pore pressure gradient (psi/ft or lb/gal), (kPa/m, g/cc). OBG = Overburden gradient (psi/ft or lb/gal), (kPa/m, g/cc). PP_N = Normal pore pressure gradient (psi/ft or lb/gal), (kPa/m, g/cc). DT_O = Observed interval transit time (msec/m). DT_N = Normal interval transit time (msec/m). x = Eaton exponent (dimensionless).

Bower’s method

The Bower’s method uses sonic velocity empirically to calculate the value of the vertical effective stress, which is then subtracted from the overburden (total vertical stress) to determine the pore pressure.

This method can be applied to predict the pore pressure caused by compaction disequilibrium or due to some source mechanism.

“Loading” method

In the “loading” method only two empirical parameters are required, if the overpressure is caused by compaction disequilibrium “loading”.

$$pp = \frac{\left(\frac{10^6 - 10^6}{DT - DT_{ml}} \right)^{(1/B)}}{depth} \tag{2}$$

The values of the two parameters can be empirically determined in the compaction trends analysis or selected based on experience in offset wells.

“Unloading” method

Further information and additional empirical parameters are required when stress is caused by the source mechanism.

The “Maximum velocity depth” parameter, d_{maxv} controls whether “unloading” has occurred or not. If $d_{maxv} > \text{depth}$, “unloading” has not occurred. If $d_{maxv} < \text{depth}$ then the assumed “unloading” behavior of pore pressure is calculated as follows:

$$PP = OBG - \frac{(\sigma_{max})^{(1-U)} \left(\frac{10^6}{DT} - \frac{10^6}{DT_{ml}} \right) \left(\frac{U}{B} \right)}{\text{depth}} \quad (3)$$

and

$$\sigma_{max} = \left(\frac{10^6}{DT_{min}} - \frac{10^6}{DT_{ml}} \right) \left(\frac{1}{B} \right)$$

where PP = Pore pressure gradient (psi/ft, lb/gal), (kPa/m, g/cc). OBG = Overburden gradient (psi/ft, lb/gal), (kPa/m, g/cc) DT = Sonic travel time (microsec/ft, microsec/m) DT_{ml} = Sonic travel time on V_{max} . A, B, U = Empirical values. V_{max} = The velocity at which unloading occurred for sediments buried at depths. d_{maxv} = Depth at which unloading has occurred. Depth = TVD in appropriate units.

In this case, the vertical effective stress of the sediment will be less than in the past and is called the “unloaded state”.

To perform this analysis, it is necessary to know the sediment's previous maximum effective stress σ_{max} , and it is necessary to determine the effective stress behavior of the sediment “unloading” velocity, which is determined by the unloading parameter, U. The value of σ_{max} is calculated from the normal compaction response and the user defined value of; and the value of U is determined empirically.

Fracture gradient (FG) prediction calculation

In predicting fracture gradient (FG) there are several methods that can be used, including: Eaton's Method, Daine's Method, and Matthew and Kelly Method.

Eaton's method

Fracture pressure is the pressure that forms the fracture, when the minimum compressive stress and tensile strength are exceeded by the pore fluid pressure. Practically speaking, the fracture pressure is the limit of pressure that a formation can withstand from a given column of mud.

Prediction of fracture pressure, LOT trend can be valid and representative using the Eaton calculation method.

$$FG = PP + (OBG - PP) \left(\frac{\nu}{1 - \nu} \right) \quad (4)$$

where FG = Fracture gradient (psi/ft or lb/gal), (kPa/m or g/cc). PP = Pore pressure gradient (psi/ft or lb/gal), (kPa/m or

g/cc). OBG = Overburden gradient (psi/ft or lb/gal), (kPa/m or g/cc). ν = Poisson's ratio (dimensionless).

Daine's method (1982)

The Daine's method in predicting the fracture gradient by superposing the horizontal tectonic stress t to the Eaton equation. Expressing in terms of stress, as “the minimum stress in the borehole that must be resisted opening and extending the existing fault”, which can be written in the following equation:

$$FG = \frac{\sigma_1 + \sigma \left(\frac{\nu}{1 - \nu} \right) + P}{\text{depth}} \quad (5)$$

where σ = Vertical effective stress. σ_1 = Superimposed tectonic stress. ν = Eaton's Poisson's ratio. P = Pore pressure.

In determining the value of the effective pressure ratio (K), Daine uses an additional parameter to describe the lithological condition due to the influence of tectonic activity. For example, there are folds and faults. Therefore, the fracture pressure value obtained from the Daine's method will depend on the lithology, depth, and tectonic activity.

Matthew and Kelly method

The Matthew and Kelly method is a fracture gradient prediction method using a variable of “matrix stress coefficient (K_i)”, equivalent to the effective stress coefficient to calculate the fracture gradient of sedimentary formations:

$$FG = PP + (OBG - PP) K_i \quad (6)$$

where FG = Fracture gradient (psi/ft or lb/gal), (kPa/m or g/cc). PP = Pore pressure (psi/ft or lb/gal), kPa/m or g/cc). OBG = Overburden gradient (psi/ft or lb/gal), kPa/m or g/cc). K_i = Matrix stress coefficient (dimensionless).

Determination of overpressure generating mechanism

The wireline log data response will show two basic criteria for the overpressure formation mechanism, namely “loading” and “unloading”.

Characteristics of loading mechanism

The wireline log shows that the porosity data is constant and the pore pressure is parallel to the lithostatic stress under top overpressure, which is based on simple assumptions, including uniform lithology, no fluid outflow, no temperature change, and no diagenesis. A pore pressure profile parallel to the lithostatic pressure associated with constant porosity is usually estimated as the young mud-rich sequences

undergoing rapid burial in sedimentary basins and is generally considered as disequilibrium compaction. The loading mechanism will show a constant trend of sonic log and density log, which is caused by the retention rate of the pore fluid compaction rate of the rock.

Accumulation of sediment causes an increase in vertical stress, or gravitational loading, which can potentially lead to the presence of overpressure due to unbalanced compaction (disequilibrium compaction). In the unbalanced compaction process, the pressure increase is the result of the competition between the fluid liberation rate and the rate of vertical compaction that occurs due to gravitational loading due to the ongoing sedimentation process.

The increase in lateral stress as a result of tectonic compression can also cause overpressure, as occurs in the disequilibrium compaction mechanism. This is also caused by gravitational loading. Sediment can be compacted horizontally in the same way as vertical compaction, but if the fluid that fills the rock pores cannot escape (migrate due to rock compaction), the pore pressure will increase and the sediment compaction rate will decrease.

Figure 4 shows the pressure depth profile and wireline log response, where overpressure is caused by loading mechanism/disequilibrium compaction (Osborne and Swarbrick 1997).

Characteristics of unloading mechanism

The unloading mechanism can cause high levels of overpressure through processes that cause load transfer from the contact between rock grains to the fluid that fills the rock pores (Swarbrick et al. 2002). The influx of pore fluids or conversion of a solid matrix to a fluid will spontaneously cause an increase in pore pressure, if the fluid that fills the rock

pores cannot escape/isolate. If some of the load on the rock grains turns into fluid, then some of the stress that was previously accommodated by the contact between the rock grains will also move to the pore fluid. In other words, the pore fluid volume increases due to load transfer. This causes an increase in pore pressure. The unloading mechanism causes a decrease in the value of the effective stress. In contrast to the loading mechanism which does not cause a decrease in the value of the effective stress, but only holds the rock to compact normally. The unloading mechanism will show a sonic log where the direction of the log response is opposite from the normal trend because the pore fluid is expanding faster than the compaction rate.

Geological processes that cause pore fluids to increase by load transfer and lead to unloading mechanism include clay diagenesis processes, such as the process of transforming smectite into illite (Lahann and Swarbrick 2011), hydrocarbon generation (Swarbrick et al 2002), and lateral transfer or vertical transfer (Bowers 1995).

Figure 5 shows the pressure depth profile and wireline log response, where overpressure is caused by unloading mechanism/fluid expansion (Osborne and Swarbrick 1997).

Mineralogy analysis method

The results obtained from measurements using the X-ray diffraction (XRD) instrument are diffractogram graphs. The diffractogram is the output which is a graph between 2θ (diffraction angle) on the X-axis versus the intensity on the Y-axis. The intensity of the continuously diffracted X-rays is recorded as an example and the detector rotates through their respective angles (Fig. 6).

A peak in intensity occurs when the mineral contains a lattice with d -spacings corresponding to X-ray diffraction

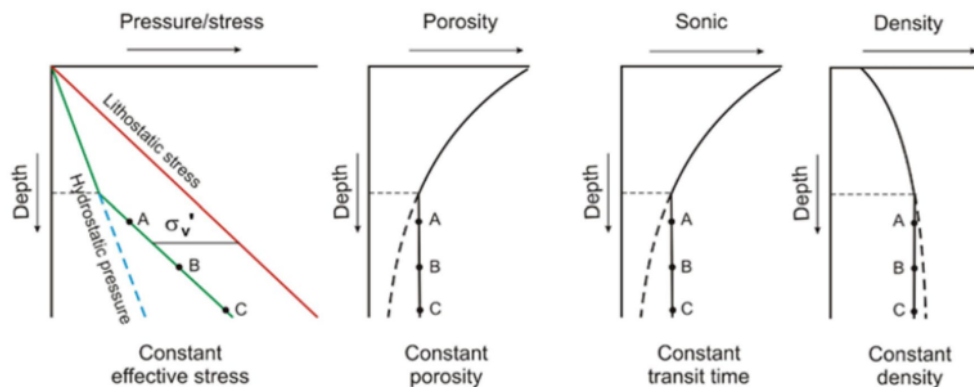


Fig. 4 The cartoon shows a depth profile and wireline log response, where overpressure is caused by loading mechanism/disequilibrium compaction: constant porosity values in the neutron porosity log, con-

stant travel time values in the sonic log, and constant density values in the density log (Osborne and Swarbrick 1997)

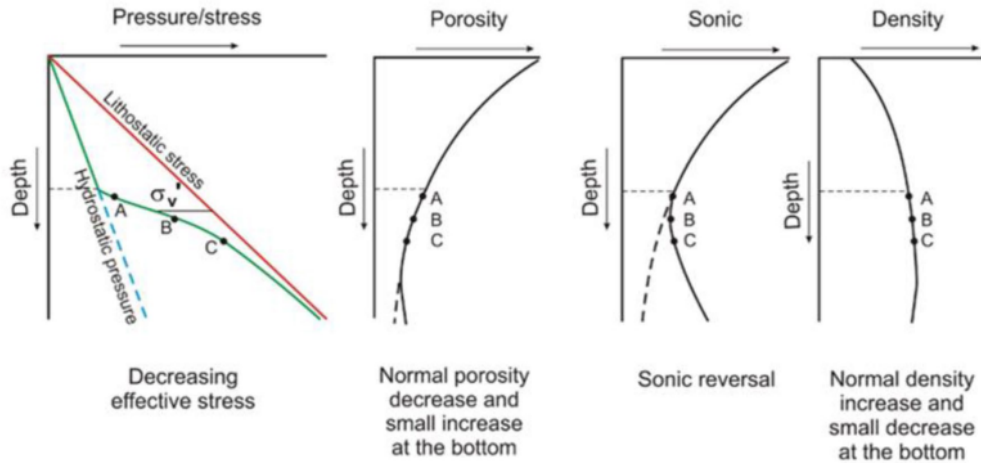
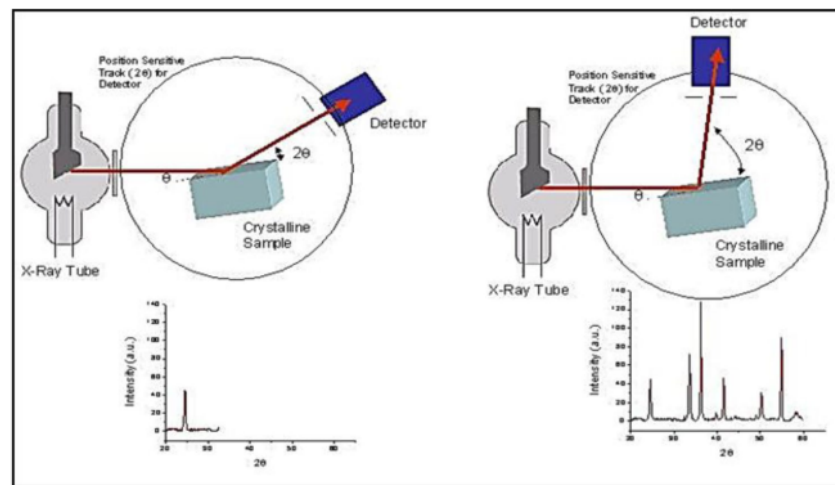


Fig. 5 The cartoon shows a depth profile and wireline log response, where overpressure is caused by the unloading mechanism: The porosity value decreases and increases slightly at the bottom of the

neutron porosity log, the travel time value is opposite in the sonic log, and the density value increases and decreases slightly at the bottom of the density log (Osborne and Swarbrick 1997)

Fig. 6 X-rays are diffracted and the detector rotates through an angle (Nurcholis 2017)



at a value of θ although each peak consists of two separate reflections ($K_{\alpha 1}$ and $K_{\alpha 2}$), at values smaller than 2θ locations to the location of the overlapping peak with $K_{\alpha 2}$ appears as a mound on the $K_{\alpha 1}$ side. Greater separation occurs at higher values of θ (theta angle).

The reading of mineral peak XRD (Fig. 7) is by reading the theta angle (deg) on the X-axis and intensity (cps) on the Y-axis at the highest peak/peak for which you want to know the name of the mineral. In determining the name of a mineral based on the measured peak (theta, deg), which is calculated by using the Bragg equation (1913), so that the d -spacing is obtained

in Angstroms (\AA). Furthermore, the d -spacing value can be used to determine the type of mineral from the Handbook of Mineralogy (Bladh et al. 2001).

After identifying the type of mineral, for example: Quartz, a semiquantitative calculation of the percent of the Quartz mineral can be carried out using a percentage calculation based on the count per second (cps) of the total identified minerals (Fig. 8).

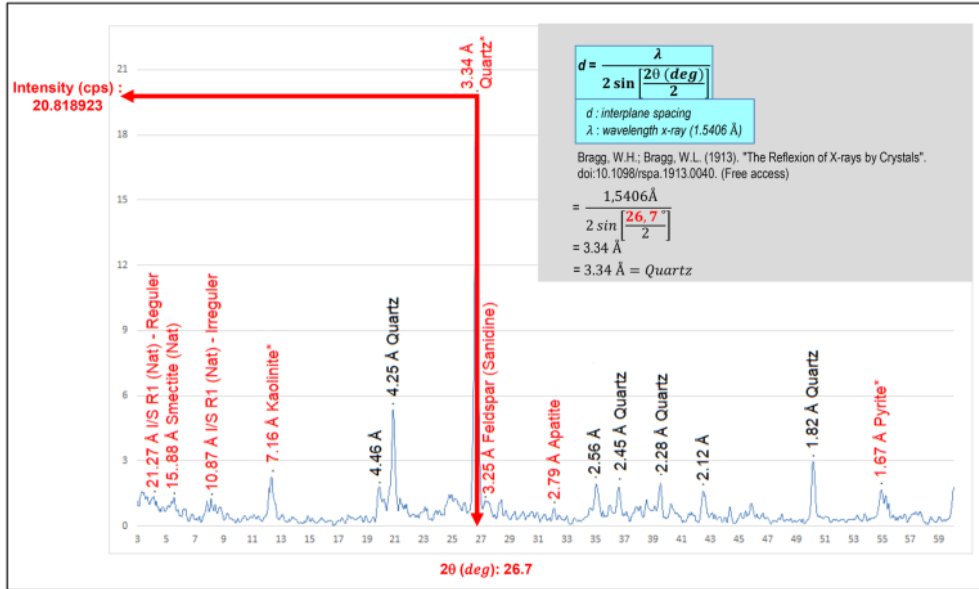


Fig. 7 Peak mineral name reading from XRD Test (Nurcholis 2017)

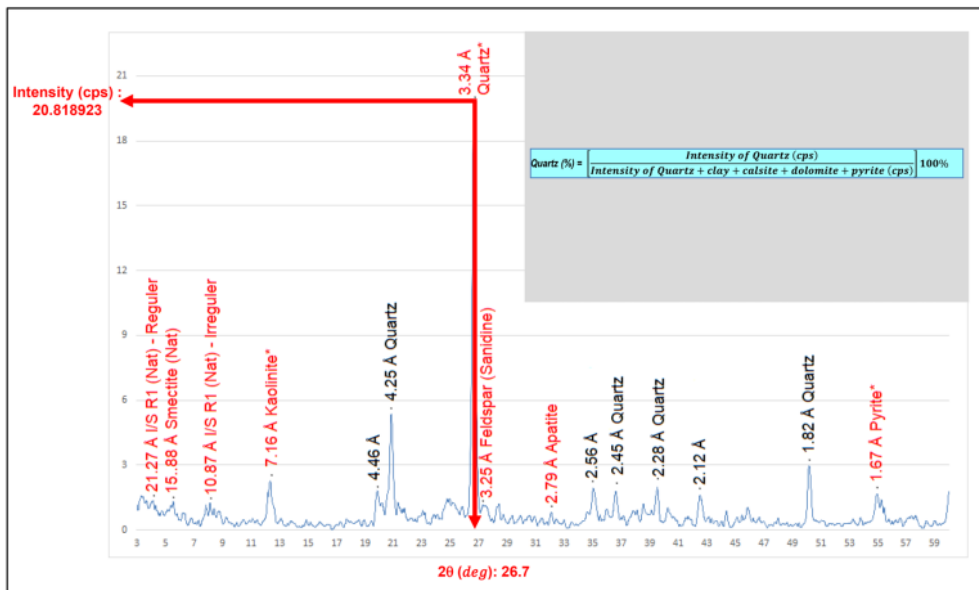


Fig. 8 Calculation of the percentage of minerals contained, for example quartz mineral (Nurcholis 2017)

Research method

The research method workflow is schematically shown in Fig. 9. The research workflow describes the research

stages starting from data collection, literature review, determination of overpressure mechanism, prediction method selection, pore pressure validation, fracture pressure estimation, fracture pressure validation, and the final result is a pore pressure fracture gradient (PPFG) model.

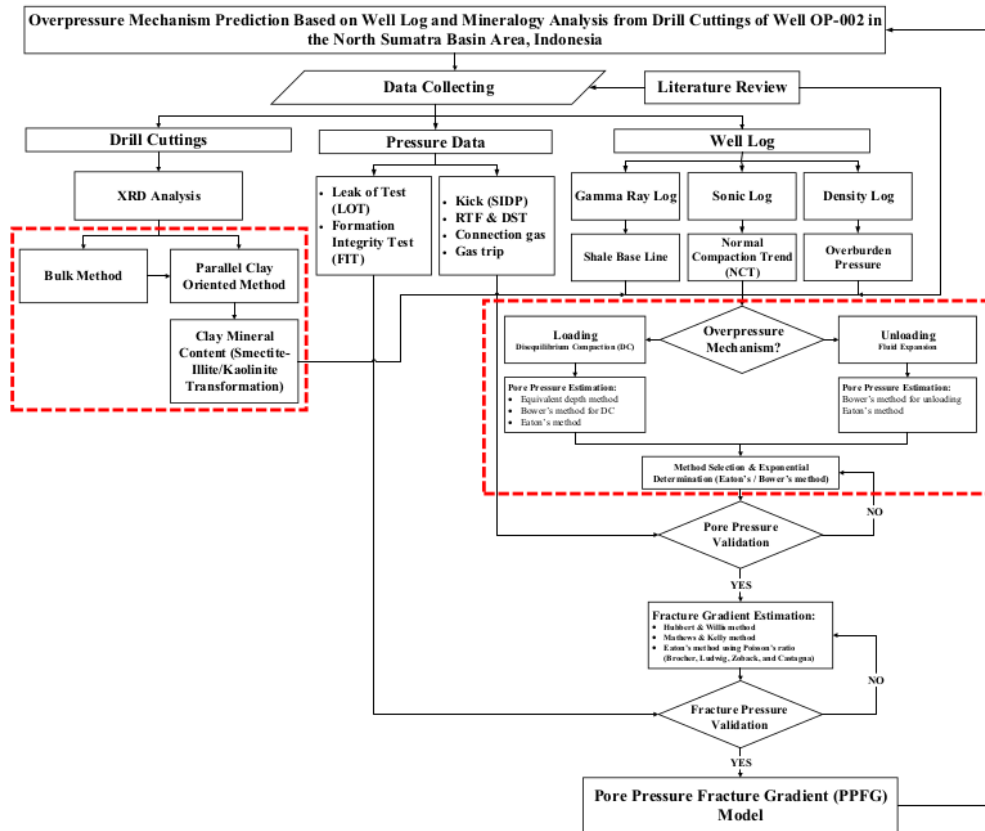


Fig. 9 The research workflow explains starting from data collection, determining the overpressure mechanism and the transformation of clay minerals which have implications for the overpressure mechanism

From the drill cuttings data were performed XRD analysis (bulk and parallel clay-oriented method) to determine bulk minerals and clay minerals and used to identify the phenomenon of clay diagenesis phenomenon (smectite to kaolinite/illite transformation) and hydrocarbon generation which has implications for the overpressure mechanism.

Results and discussion

Wireline log response analysis

The response of wireline log data of well NSE-001 based on the normal compaction trend (NCT) shows that there are two types of overpressure mechanisms, namely loading and unloading (Fig. 10). The loading and unloading intervals are detailed in Table 2. The loading mechanism is shown by a constant trend of sonic log and density log, which is caused by rapid sedimentation (disequilibrium compaction).

Meanwhile, the unloading mechanism is shown by trend of sonic log and density log in the opposite direction from the normal trend response, which is thought to be due to the influence of fluid expansion, caused by the smectite to kaolinite/illite transformation (clay diagenesis) and hydrocarbon generation.

From the measurement data of well NSE-001 with Mean Sea Level 0 m, Drill Floor 34.35 m above Datum, the NSE-001 Max Recorded Bottom Hole Temperature (BHT) well is 126.67 °C at a depth of 2565.35 mMD, so it can be estimated that the temperature of 100 °C is at a depth of 2035.71 mMD (Fig. 10).

In the North Sumatra Basin, there is an overpressure phenomenon in the Middle Miocene Lower Baong and Keutapang formations at depth intervals of 4000–8000 ft, which is caused by rapid sedimentation/burial of sediments (Aziz and Bolt 1984). This can be seen very clearly in the wireline log data response of well NSE-001 based on the normal compaction trend (NCT), where at a depth interval

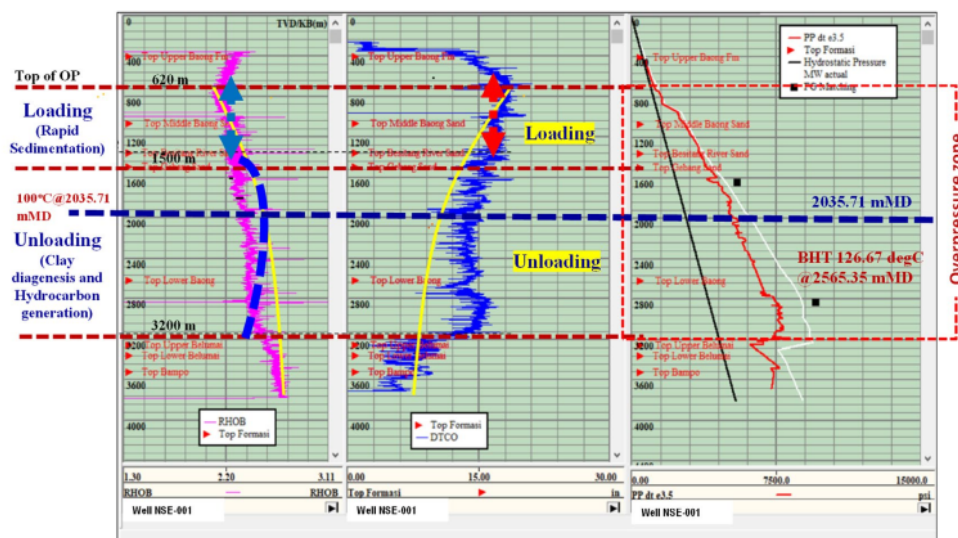


Fig. 10 The response of the wireline log data of well NSE-001 based on the normal compaction trend (NCT) shows two types of overpressure mechanisms (loading and unloading)

Table 2 Loading and unloading intervals based on the response of the wireline log data of well NSE-001 to the normal compaction trend (NCT)

Depth interval (mTVD)	Overpressure formation zone	Overpressure mechanism
620–1500	From the Middle Baong Formation to the top Gebang Sand Formation	Loading
1500–3200	From the Top Gebang Sand Formation to the Top Upper Belumain Formation	Unloading

of 620–1500 mTVD (from the Middle Baong Formation to the Top Gebang Sand Formation) indicating that the travel time in the sonic log is relatively constant, and referred to as the loading mechanism (Fig. 10).

Mineralogy analysis

The very thick rapid sedimentation of the Baong Formation is coupled with a high thermal gradient, so it is believed to have implications for the presence of overpressure in the North Sumatra Basin (Aziz and Bolt 1984).

Based on the crossplot density (gr/cc) versus transit time (msec/m) it shows that the Upper Baong Formation is located in the smectite rich mud rock as a low overpressure zone, while the overpressure is present in the Lower Baong Formation which is located in the kaolinite + illite-rich. Thus, it can be concluded that the overpressure in the

Lower Baong Formation is caused by the unloading mechanism, due to the smectite to illite/kaolinite transformation (Hutasoit et al. 2013). Overpressure characteristics in the Tamiang Sub-basin, North Sumatra Basin indicates that there are two overpressure mechanisms, namely the loading mechanism caused by the rapid sedimentation rate in the basin and the unloading mechanism caused by clay diagenesis and hydrocarbon generation (Yosandian et al. 2014).

The results of XRD analysis of drill cuttings of well NSE-001 for bulk analysis (Table 3) show the significant presence of sillimanite and kaliophilite minerals at depth intervals of 2200–3820 mMD (Gebang Sand Formation, Lower Baong Formation, Belumai Formation, and Bampo Formation) which has implications for clay diagenesis (smectite to illite/kaolinite transformation) and hydrocarbon generation (Buntoro et al 2020). From the results of clay analysis of drill cuttings at depths ranging from 2200 mMD downwards with temperature conditions reaching 100 °C (Table 4), it shows that the percentage of smectite mineral content is low (low smectite content), while the total content of kaolinite + illite is very significant (high kaolinite + illite content). The presence of significant kaolinite + illite minerals is an alteration product (Fig. 11) which has implications for the overpressure mechanism in the well NSE-001.

Based on mineralogy analysis (XRD) at depth intervals of 2200–3820 mMD (from the Gebang Sand Formation to the Bampo Formation), both bulk analysis and clay analysis showed a correlation with the response of the wireline log data of well NSE-001 to the normal compaction trend (NCT). The presence of sillimanite and kaliophilite minerals

Table 3 Result of XRD analysis (Bulk) of drill cuttings of well NSE-001

No	Depth (mMD)	Main Mineral			Other Mineral					
		Quartz (%)	Calcite (%)	Clay (%)	Feldspar (%)	Apatite (%)	Dolomite (%)	Pyrite (%)	Sillimanite (%)	Kaliohillite (%)
1	2200-2230	33.43	2.99	19.78	1.86	5.51	5.52	3.33	19.52	8.06
2	2230-2260	29.49	2.64	21.26	3.17	5.85	7.69	3.29	13.95	12.67
3	2260-2290	38.07	2.66	17.85	3.97	5.49	6.00	3.76	11.58	10.62
4	2290-2320	25.11	2.39	21.68	2.53	5.88	5.62	3.62	21.55	11.62
5	2320-2350	37.31	2.76	19.12	3.34	5.51	5.02	4.36	11.71	10.88
6	2350-2380	35.67	0.00	20.92	2.60	6.17	5.59	3.21	15.10	10.74
7	2380-2410	32.35	0.00	18.55	4.35	5.91	5.91	3.89	16.04	13.84
8	2410-2440	27.45	2.22	18.03	0.00	7.23	7.28	3.39	18.30	16.10
9	2440-2470	37.79	2.65	15.13	2.27	5.61	5.29	4.18	13.45	13.63
10	2470-2500	36.54	2.13	17.64	2.83	4.64	5.70	4.08	15.13	11.30
11	2500-2530	34.57	2.91	21.16	3.01	7.28	5.27	3.22	13.33	9.24
12	2530-2560	26.70	2.15	18.30	2.81	10.71	7.22	4.13	16.73	11.25
13	2560-2590	34.64	2.38	19.70	3.26	6.44	5.07	3.18	14.49	10.84
14	2590-2620	37.79	1.95	18.34	2.53	5.87	4.82	3.37	12.99	9.23
15	2620-2650	38.02	2.02	13.15	3.24	6.40	5.45	3.67	16.28	8.95
16	2650-2680	40.83	1.73	15.87	2.38	5.76	5.15	3.51	13.90	10.88
17	2680-2710	38.89	2.97	16.59	2.80	5.93	4.56	3.14	11.80	9.01
18	2710-2740	40.99	2.70	20.67	0.00	4.76	5.10	4.24	10.68	9.51
19	2740-2770	35.84	3.18	20.48	2.84	4.37	5.61	4.06	9.95	9.49
20	2770-2800	34.68	0.00	20.45	0.00	5.58	6.06	3.99	14.92	10.99
21	2800-2830	30.73	0.00	16.22	0.00	8.72	7.19	4.86	15.59	13.36
22	2830-2860	22.53	3.69	15.73	0.00	7.04	6.11	3.97	23.28	14.73
23	2860-2890	28.90	3.52	14.40	0.00	7.26	7.20	5.38	17.46	13.52
24	2890-2920	25.72	3.62	19.08	0.00	8.61	7.00	3.39	16.45	13.42
25	2920-2950	21.41	3.02	16.62	6.45	6.36	6.14	3.56	19.69	10.93
26	2950-2980	42.12	0.00	15.24	0.00	7.42	6.75	2.94	14.25	11.28
27	2980-3010	32.08	6.38	17.03	0.00	6.75	5.57	4.85	11.80	15.54
28	3010-3040	25.71	2.87	16.60	0.00	13.67	5.70	2.76	18.10	10.49
29	3040-3070	33.79	3.62	17.95	0.00	5.86	6.40	2.98	14.18	10.60
30	3070-3100	30.07	8.81	19.78	0.00	4.66	5.73	3.59	15.75	11.61
31	3100-3130	26.65	18.48	19.05	0.00	5.38	5.19	3.12	13.04	9.09
32	3130-3160	24.36	15.98	19.41	0.00	6.56	7.54	3.69	12.08	10.40
33	3160-3190	21.31	9.33	18.33	0.00	5.42	4.33	4.74	15.41	11.05
34	3190-3220	29.28	19.74	15.87	0.00	4.96	4.81	2.42	12.10	10.82
35	3220-3250	35.81	13.78	14.81	0.00	5.70	5.07	3.12	12.01	9.69
36	3250-3280	34.96	21.00	12.48	0.00	3.71	4.50	2.72	11.15	9.48
37	3280-3310	44.49	10.80	12.15	0.00	5.86	5.56	2.26	10.41	8.47
38	3310-3340	48.61	11.92	12.22	0.00	2.95	5.29	3.29	7.31	8.42
39	3340-3370	49.69	5.14	17.85	0.00	3.15	4.04	3.65	8.93	7.54
40	3370-3400	49.88	0.00	20.62	0.00	3.21	5.35	4.82	8.87	7.26
41	3400-3430	59.87	0.00	12.88	1.21	2.99	3.34	3.64	7.52	5.31
42	3430-3460	57.32	0.00	19.46	1.74	3.44	0.00	4.79	7.03	6.98
43	3460-3490	57.83	0.00	17.66	0.00	5.31	0.00	3.80	8.57	6.82
44	3490-3520	48.34	0.00	19.86	0.00	4.97	3.99	3.84	10.55	8.45
45	3520-3550	43.08	0.00	24.52	0.00	4.59	5.25	4.47	9.95	8.14
46	3550-3580	52.13	0.00	17.53	0.00	3.59	4.59	4.57	9.23	8.36
47	3580-3610	56.60	0.00	12.07	5.99	4.54	0.00	3.58	9.48	7.74
48	3610-3640	53.03	0.00	17.96	0.00	4.23	4.46	3.87	8.77	7.68
49	3640-3670	50.33	0.00	15.18	0.00	4.15	5.16	4.69	10.83	9.36
50	3670-3700	51.16	0.00	16.84	0.00	4.85	4.00	3.99	8.85	7.30
51	3700-3730	57.23	0.00	13.70	0.00	3.99	4.78	3.17	9.55	7.57
52	3730-3760	56.22	0.00	14.41	0.00	4.37	4.37	3.67	9.08	7.88
53	3760-3790	53.67	0.00	16.48	0.00	3.83	4.41	3.71	11.01	6.89
54	3790-3820	54.89	0.00	15.98	0.00	3.33	4.09	4.54	10.62	6.54

in bulk analysis contributed to the generation of hydrocarbons, and clay analysis showed that the mineral content of kaolinite+ illite as alteration products (clay diagenesis) was higher than the mineral content of smectite. It can be concluded that the depth interval of 1500 m to 3200 mMD is an overpressure zone with an unloading mechanism, which is characterized by fluid expansion caused by clay diagenesis and the possibility of hydrocarbon generation.

Summary and conclusions

- Based on the response of the wireline log data of well NSE-001 to the normal compaction trend (NCT), it shows that there are two types of overpressure mechanisms, namely loading and unloading. At a depth

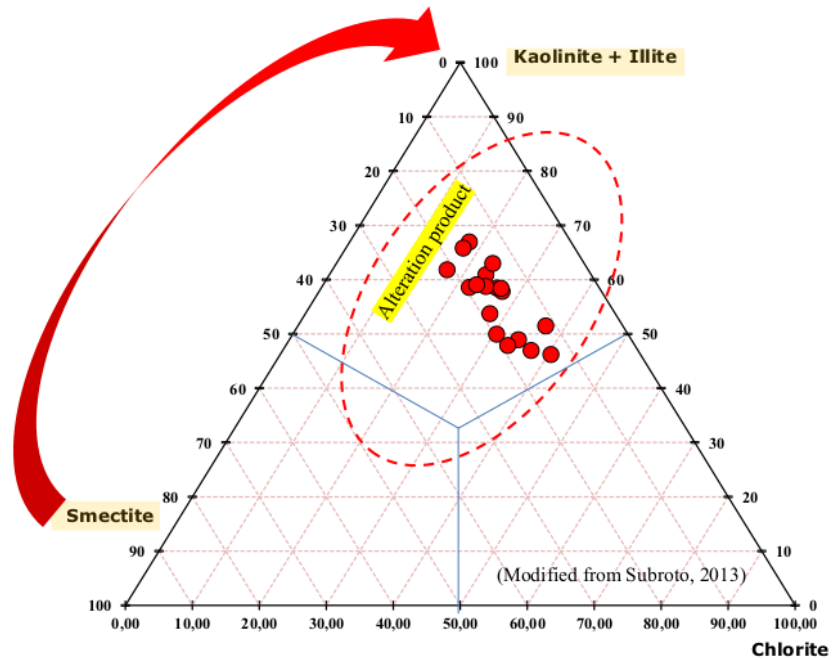
interval of 620–1500 mMD (from the Middle Baong Sand Formation to the Upper Gebang Sand Formation), where the travel time of the sonic log is relatively constant with response to the normal compaction trend (NCT), and is referred to as a loading mechanism caused by rapid sedimentation. Furthermore, at a depth interval of 1500–3200 mMD (from the Upper Gebang Sand Formation to the Upper Top Bawah Formation) the response of the wireline log data of well NSE-001 to normal compaction (NCT), where the travel time value is opposite to the sonic log, and the density value increases and decreases slightly at the bottom of the density log. Based on the response from the wireline log to the NCT, this overpressure depth interval is referred to as the unloading mechanism.

Table 4 Result of XRD analysis (Clay mineral) of drill cuttings of well NSE-001

No	Depth (mMD)	Clay Mineral			
		Kaolinite (%)	Illite (%)	Smectite (%)	Chlorite (%)
100°C @2035.71 mMD					
1	2200-2230	44,0	16,8	15,5	23,4
2	2290-2320	40,7	17,7	15,3	26,3
3	2380-2410	48,2	18,7	15,2	17,9
Gebang Sand Fm.					
4	2440-2470	39,8	18,0	14,8	27,4
5	2530-2560	46,6	19,2	16,7	17,6
6	2590-2620	33,4	13,5	15,9	37,0
7	2710-2740	31,7	19,7	11,6	37,0
8	2730-2800	37,4	21,2	19,4	22,1
9	2860-2890	32,2	16,7	16,9	34,2
Lower Baong Fm.					
10	2950-2980	29,7	16,5	13,4	40,4
11	3070-3100	40,5	18,2	16,8	24,4
12	3190-3220	39,8	22,0	21,1	17,1
13	3250-3280	35,0	14,9	19,6	30,5
14	3340-3370	40,7	17,7	14,7	26,9
Belumai Fm.					
15	3430-3460	40,9	18,1	18,1	22,9
16	3520-3550	42,5	20,5	13,7	23,4
Bampo Fm.					
17	3670-3700	31,1	16,7	19,0	33,2
18	3760-3790	33,2	20,5	18,8	27,6

high kaolinite+illite content low smectite content

Fig. 11 Ternary diagram of XRD analysis (Clay mineral) of drill cuttings of well NSE-001



- The results of mineralogy analysis of drill cuttings at depth intervals of 2200–3820 mMD showed the presence of sillimanite and kaliophilite minerals in bulk analysis that contributed to the generation of hydrocarbon, while clay analysis showed that the mineral content of kaolinite + illite as alteration product (clay diagenesis)

was higher than the mineral content of smectite. It can be concluded that the depth interval of 1500 m to 3200 mMD is an overpressure zone with an unloading mechanism, which is characterized by fluid expansion caused by clay diagenesis and the possibility of hydrocarbon generation.

- Rapid sedimentation in the development of the Lower Baong Formation and Upper Baong Formation as thick and massive shale sequences in the North Sumatra Basin is the main factor for the overpressure zone. Based on the Bottom Hole Temperature (BHT) measurement in the well NSE-001, it is estimated that a temperature of 100 °C at a depth of 2035.71 mMD will have implications for clay diagenesis and hydrocarbon generation which contributes to overpressure.

Acknowledgements The authors wish to thank LPPM UPN Veteran Yogyakarta, Upstream Innovation–Pertamina Hulu Energy, and Exploration Drilling–Pertamina EP. This work was carried out with the support of LPPM UPN Veteran Yogyakarta who has provided funding for this research, Upstream Innovation–Pertamina Hulu Energy which has collaborated in XRD and geomechanical analysis studies, and Drilling Exploration–Pertamina EP for data contributions and publication permits.

Author contribution AB as the Lead researcher (Geoscientist) who summarizes the research results for writing this paper; BR as a member of the researcher (Geologist) who makes geological analysis in this research; AHL (Geothermal Engineer) & DA (Petroleum Engineers) as research members who conducted wireline log and mineralogy analysis; EFF (Geomechanics specialist) as partner from the oil and gas industry in the study of geomechanical and XRD analysis; EA (Drilling Expert–Pertamina EP) who has provided data and gave permission for research and publication; all authors had approved the final version.

Funding This work was funded by LPPM UPN “Veteran” Yogyakarta, Indonesia (Grant Number B/41/UN.62/PT/IV/2021). Upstream Innovation – Pertamina Hulu Energy which has collaborated in XRD and geomechanical analysis studies, and Drilling Exploration – Pertamina EP for data contributions and publication permits.

Declarations

3
Conflict of interest The authors declare no conflict of interest regarding the publication of this paper.

Open Access This article is licensed under a Creative Commons Attribution 4.0 International License, which permits use, sharing, adaptation, distribution and reproduction in any medium or format, as long as you give appropriate credit to the original author(s) and the source, provide a link to the Creative Commons licence, and indicate if changes were made. The images or other third party material in this article are included in the article's Creative Commons licence, unless indicated otherwise in a credit line to the material. If material is not included in the article's Creative Commons licence and your intended use is not permitted by statutory regulation or exceeds the permitted use, you will need to obtain permission directly from the copyright holder. To view a copy of this licence, visit <http://creativecommons.org/licenses/by/4.0/>.

References

- Aziz A and Bolt LH (1984) Occurrence and detection of abnormal pressures from geological and drilling data, North Sumatra Basin. In: Proceedings 13th Indonesian petroleum association annual convention, p 195–220, Jakarta, <https://doi.org/10.29118/ipa.1191.195.220>
- Barber AJ et al (2005) Sumatra geology, resources, and tectonic evolution. Geological Society Memoir IX

- Barliana A et al (1999) Changing perceptions of a carbonate gas reservoir: alur siwah field, aceh timur sumatra. Indonesian Petroleum Association
- Basuki D (2019) Introduction to petroleum geomechanics. SPE UPN “Veteran” Yogyakarta student chapter course, p 65, https://www.researchgate.net/publication/356159891_2019_Introduction_to_Petroleum_Geomechanics_-_SPE_UPN_Yogyakarta
- Bladh KW et al (2001) Handbook of mineralogy. Mineralogical Society of America
- Bowers GL (1995) Pore pressure estimation from velocity data: accounting for overpressure mechanisms besides undercompaction. SPE Drill Complet 10(02):89–95. <https://doi.org/10.2118/27488-PA>
- Bragg WL (1913) The diffraction of X-rays by crystals. Zeitschrift Fur Physikalische Chemie 228(10–12):957–968. <https://doi.org/10.1515/zpch-2014-9027>
- Buntoro A et al (2020) Correlation of sillimanite & kaliophilite minerals, TOC, Ro, and MBT from drill cutting of well BS-03 in the development of shale hydrocarbon, brownshale formation, bengkalis trough, Central Sumatra Basin, Indonesia. Open J Yangtze Oil Gas 5:216–230
- Eaton BA (1975) The equation for geopressure prediction from well logs. SPE Ann Tech Conf Exhib. <https://doi.org/10.2118/5544-MS>
- Gurning JCH, Ramdhan AM (2017) Metode Seismic Pore Pressure Untuk Penyebaran Tekanan Luap Di Blok Aru Cekungan Sumatra Utara. Bull Geol 1(2):123–133
- Harding TP (1974) Petroleum traps associated with wrench faults. Bull Am Assoc Petrol Geol 58(7):1290–1304
- Hottman GE and Johnson RK (1965) Estimation of formation pressures from log-derived shale properties. In: SPWLA 6th annual logging symposium 2:717–722
- Lahann RE, Swarbrick RE (2011) Overpressure generation by load transfer following shaleframework weakening due to smectite diagenesis. Geofluids 11:362–375
- Pulungono A et al (1992) Pre-tertiary and tertiary fault systems as a framework of the south sumatra basin. In: Proceedings Indonesian petroleum association.
- Hutasoit LM et al (2013) Overpressure characteristics in pertamina's area in the North Sumatra Basin. In: 37th Indonesian petroleum association annual convention and exhibition p 101–117
- Matthews WR, Kelly J (1967) How to predict formation pressure and fracture gradient. Oil Gas J 65:92–1066
- McClendon R (1971) Measurement of formation pressure from drilling data. In: SPE annual technical conference and exhibition
- Moulds PJ (1989) Development of the bengkalis depression, central sumatra and its subsequent deformation—a model for other sumatran grabens?. In: Indonesian petroleum association proceeding, p 217–246
- Nurcholis M (2017) Proses pembuatan preparasi sampel dan running XRD. Lab XRD UPN Veteran, Yogyakarta
- O’Conner S et al (2011) Geologically driven pore fluid pressure models and their implications for petroleum exploration introduction to thematic set. Geofluids 11(4):343–348
- Osborne MJ, Swarbrick RE (1997) Mechanisms for generating overpressure in sedimentary basins: a reevaluation. AAPG Bull 81(6):1023–1041
- Pennebaker ES (1968) An engineering interpretation of seismic data. In: SPE annual technical conference and exhibition 2165
- Satyana AH (2009) Petroleum geology of Indonesia : current knowledge regular HAGI course. HAGI Course
- Storvoll V, Brevik I (2008) Identifying time, temperature, and mineralogical effects on chemical compaction in shales by rock physics relations. Lead Edge 27(6):750–756
- Subroto E et al (2013) Integrated geochemical, geomechanical and geological (3G) study of lower baong shale formation for preliminary shale gas prospectivity in the North Sumatra Basin. In: Society of petroleum engineers - Asia Pacific unconventional resources

- conference and exhibition 2013: delivering abundant energy for a sustainable future p 297–311, <https://doi.org/10.2118/167027-ms>.
- Swarbrick R, Osborne M, Yardley G (2002) Comparison of overpressure magnitude resulting from the main generating mechanisms. AAPG Memoirs 76:1–12
- Syaiful M et al (2020) Wireline log responses, mudweight, clay mineralogy, and implied overpressure condition: insights from aru field, North Sumatra Basin. Indones J Geosci 7(2): 105–119
- Yosandian HH et al (2014) Overpressure characteristic in the Langkat field, North Sumatra Basin, Indonesia. Int Conf Geol Environ Sci 73:9
- Zamora M (1974) Practical analysis of drilling mud flow in pipes and annuli. In: SPE annual technical conference and exhibition SPE-4976-M.

Publisher's Note Springer Nature remains neutral with regard to jurisdictional claims in published maps and institutional affiliations.

Overpressure mechanism prediction based on well log and mineralogy analysis from drill cuttings of well NSE-001 in the North Sumatra Basin area, Indonesia

ORIGINALITY REPORT

7%

SIMILARITY INDEX

7%

INTERNET SOURCES

2%

PUBLICATIONS

2%

STUDENT PAPERS

PRIMARY SOURCES

1

www.spgindia.org

Internet Source

3%

2

docplayer.net

Internet Source

2%

3

shura.shu.ac.uk

Internet Source

2%

Exclude quotes On

Exclude matches < 2%

Exclude bibliography On